

# LHC signals of the next-to-lightest scalar Higgs state of the NMSSM in the $4\tau$ decay channel

M. M. Almarashi

*Physics Department, Faculty of Science, Taibah University  
P. O. Box 344, Medina, KSA*

## Abstract

We study the  $a_1 a_1$  and  $Z a_1$  decay channels of the next-to-lightest CP-even Higgs boson  $h_2$  of the NMSSM at the LHC, where the  $h_2$  is produced in gluon fusion. It is found that while the  $h_2$  discovery is impossible through the latter channel, the former one in the  $4\tau$  final state is a promising channel to discover the  $h_2$  with masses up to around 250 GeV at the LHC. Such a discovery of the  $h_2$  is mostly accompanied with a light  $a_1$ , which is a clear evidence for distinguishing the NMSSM from the MSSM since such a light  $a_1$  is impossible in the MSSM.

## 1 Introduction

The discovery of the standard model (SM)-like Higgs boson with a mass around 125 GeV at the LHC [1–4] can be accommodated in the framework of the next-to-minimal supersymmetric standard model (NMSSM) [5–16] without much fine tuning, and as a consequence it has acquired increasing attention. In this model one Higgs singlet field is added to the two MSSM-type Higgs doublets in order to give a natural explanation of the  $\mu$ -problem of the MSSM [17]. So, the Higgs sector of the NMSSM is phenomenologically richer than that of the MSSM due to the existence of this extra Higgs singlet.

The Higgs spectrum of the NMSSM after electroweak symmetry breaking contains seven Higgs mass states, assuming CP-conservation: two pseudoscalar Higgses  $a_{1,2}$  ( $m_{a_1} < m_{a_2}$ ), three scalar Higgses  $h_{1,2,3}$  ( $m_{h_1} < m_{h_2} < m_{h_3}$ ) and a pair of charged Higgses  $h^\pm$ . Following the discovery of the SM-like Higgs boson in 2012, the observation of additional Higgs bosons, if they exist, would point to the existence of supersymmetric extensions of the SM. In the NMSSM framework, the search for light Higgs bosons has been done by many authors, aiming to establish the so-called a ‘no-lose theorem’ of the NMSSM stating that one or more of the Higgs bosons of the NMSSM should be discovered at the LHC throughout the entire NMSSM parameter space [18–27]. All these studies were performed before the discovery of the Higgs boson at the LHC in 2012. Many studies have also been done on the discovery potential of other Higgs bosons of the NMSSM following the 2012 discovery [28–51].

One of the interesting feature of the NMSSM is that Higgs-to-Higgs decays are dominant over large regions of parameter space if they are kinematically allowed. The importance of such decays in the framework of the NMSSM has long been emphasized in the literature, see, e.g., Ref. [52]. It was found that Vector Boson Fusion (VBF) could be a suitable production channel to detect  $h_{1,2} \rightarrow a_1 a_1$  at the LHC, in which the Higgs pair decays into  $jj\tau^+\tau^-$

[19]. Both the Vector Boson Fusion and Higgs-strahlung production mechanisms could also be useful to discover such Higgses in the  $4\tau$  final states [53]. Furthermore, some scope could be afforded by  $4\mu$  and  $2\tau 2\mu$  signatures in the gluon-fusion production channel [22, 54]. Higgs production in association with a  $b\bar{b}$  pair could also be a good means to search for the  $h_{1,2} \rightarrow Za_1$  at the LHC [55]. All these studies were performed prior to the Higgs discovery in 2012.

In this paper, we study the LHC discovery potential for the next-to-lightest CP-even Higgs boson  $h_2$ , which is not a SM-like Higgs, decaying either into two light CP-odd Higgs bosons  $a_1a_1$  or into a light  $a_1$  and a gauge boson  $a_1Z$  through the gluon fusion  $gg \rightarrow h_2$  in the  $4\tau$  final state in the NMSSM framework. We calculate the signal rates of the two processes  $gg \rightarrow h_2 \rightarrow a_1a_1 \rightarrow 4\tau$  and  $gg \rightarrow h_2 \rightarrow Za_1 \rightarrow 4\tau$  to examine whether or not there are some regions of NMSSM parameter space where the  $h_2$  and  $a_1$  states can simultaneously be observed at the LHC.<sup>1</sup> We perform a partonic signal-to-background analysis of the  $h_2$  production. It is found that there are parameter regions of the NMSSM where the  $h_2$  and  $a_1$  signals may be found at the LHC through the process  $gg \rightarrow h_2 \rightarrow a_1a_1 \rightarrow 4\tau$ .

The paper is planned as follows. In the next section we briefly discuss the Higgs sector of the NMSSM, describing the NMSSM parameter space scans performed under current constraints. In section 3 we present the inclusive production rates of the  $h_2$  at the LHC in the  $4\tau$  final states as well as signal-to-background analysis for some benchmark points. Finally, conclusions are given in section 4.

## 2 The Higgs sector of the NMSSM

The scale invariant superpotential of the NMSSM in terms of the usual two MSSM-type Higgs doublets superfields  $\hat{H}_u$  and  $\hat{H}_d$  as well as the singlet one  $\hat{S}$  is given by [8, 9]

$$W_{NMSSM} = \text{MSSM Yukawa terms} + \lambda \hat{S} \hat{H}_u \hat{H}_d + \frac{1}{3} \kappa \hat{S}^3, \quad (1)$$

where both  $\lambda$  and  $\kappa$  are dimensionless couplings. The term  $\lambda \hat{S} \hat{H}_u \hat{H}_d$  is introduced to solve the  $\mu$ -problem of the MSSM superpotential. When the singlet superfield develops a vacuum expectation value (VEV)  $\langle S \rangle = \frac{1}{\sqrt{2}} v_s$  upon spontaneous symmetry breaking, an ‘effective’  $\mu$ -parameter given by  $\mu_{\text{eff}} = \lambda \langle S \rangle$  of the order of the electroweak scale will be automatically generated. The last term of the above equation is introduced to avoid the Peccei-Quinn symmetry [56, 57]. The soft breaking terms for both the doublet and singlet fields read

$$V_{NMSSM} = m_{H_u}^2 |H_u|^2 + m_{H_d}^2 |H_d|^2 + m_S^2 |S|^2 + \left( \lambda A_\lambda S H_u H_d + \frac{1}{3} \kappa A_\kappa S^3 + \text{h.c.} \right), \quad (2)$$

where  $A_\lambda$  and  $A_\kappa$  are the trilinear coupling parameters of the order of SUSY mass scale  $m_{\text{SUSY}}$ .

---

<sup>1</sup>We do not consider the case of both  $b\bar{b}b\bar{b}$  and  $b\bar{b}\tau^+\tau^-$  final states because these channels are burdened by large SM backgrounds.

The physical Higgs bosons arise after the Higgs fields acquire vacuum expectation values (VEVs),  $\langle H_u \rangle = \frac{1}{\sqrt{2}}v_u$ ,  $\langle H_d \rangle = \frac{1}{\sqrt{2}}v_d$  and  $\langle S \rangle = \frac{1}{\sqrt{2}}v_s$ , and eliminating the Goldstone boson states. As a result, the potential has terms for the non-zero mass modes for the scalar fields  $S_i (i = 1, 2, 3)$ , pseudoscalar fields  $P_i (i = 1, 2)$  and charged fields  $h^\pm$  given by

$$V_{mass} = \frac{1}{2}(S_1 \ S_2 \ S_3)\mathcal{M}_S \begin{pmatrix} S_1 \\ S_2 \\ S_3 \end{pmatrix} + \frac{1}{2}(P_1 \ P_2)\mathcal{M}_P \begin{pmatrix} P_1 \\ P_2 \end{pmatrix} + m_{h^\pm}^2 h^+ h^-. \quad (3)$$

One can obtain physical mass eigenstates with tree-level masses as follows. First, the elements of the mass matrix for the CP-even Higgs states at tree-level are given by [58]

$$\mathcal{M}_{S11} = m_A^2 + \left( m_Z^2 - \frac{1}{2}(\lambda v)^2 \right) \sin^2 2\beta, \quad (4)$$

$$\mathcal{M}_{S12} = -\frac{1}{2} \left( m_Z^2 - \frac{1}{2}(\lambda v)^2 \right) \sin 4\beta, \quad (5)$$

$$\mathcal{M}_{S13} = -\frac{1}{2} \left( m_A^2 \sin 2\beta + 2 \frac{\kappa \mu_{\text{eff}}^2}{\lambda} \right) \left( \frac{\lambda v}{\sqrt{2} \mu_{\text{eff}}} \right) \cos 2\beta \quad (6)$$

$$\mathcal{M}_{S22} = m_Z^2 \cos^2 2\beta + \frac{1}{2}(\lambda v)^2 \sin^2 2\beta, \quad (7)$$

$$\mathcal{M}_{S23} = \frac{1}{2} \left( 4\mu_{\text{eff}}^2 - m_A^2 \sin^2 2\beta - \frac{2\kappa \mu_{\text{eff}}^2 \sin 2\beta}{\lambda} \right) \frac{\lambda v}{\sqrt{2} \mu_{\text{eff}}} \quad (8)$$

$$\mathcal{M}_{S33} = \frac{1}{8} m_A^2 \sin^2 2\beta \frac{\lambda^2 v^2}{\mu_{\text{eff}}^2} + 4 \frac{\kappa^2 \mu_{\text{eff}}^2}{\lambda^2} + \frac{\kappa A_\kappa \mu_{\text{eff}}}{\lambda} - \frac{1}{4} \lambda \kappa v^2 \sin 2\beta, \quad (9)$$

where  $m_A^2 = \sqrt{2} \frac{\mu_{\text{eff}}}{\sin 2\beta} \left( A_\lambda + \frac{\kappa \mu_{\text{eff}}}{\lambda} \right)$ ,  $\tan \beta = \frac{v_u}{v_d}$  and  $v^2 = v_u^2 + v_d^2$ .

Second, the elements of the mass matrix for the CP-odd Higgs states at tree-level are [58]

$$\mathcal{M}_{P11} = m_A^2, \quad (10)$$

$$\mathcal{M}_{P12} = \frac{1}{2} \left( m_A^2 \sin 2\beta - 6 \frac{\kappa \mu_{\text{eff}}^2}{\lambda} \right) \frac{\lambda v}{\sqrt{2} \mu_{\text{eff}}}, \quad (11)$$

$$\mathcal{M}_{P22} = \frac{1}{8} \left( m_A^2 \sin 2\beta + 6 \frac{\kappa \mu_{\text{eff}}^2}{\lambda} \right) \frac{\lambda^2 v^2}{\mu_{\text{eff}}^2} \sin 2\beta - 3 \frac{\kappa \mu_{\text{eff}} A_\kappa}{\lambda}. \quad (12)$$

Third, the mass of charged Higgs fields at tree-level is given by [58]

$$m_{h^\pm}^2 = m_A^2 + m_W^2 - \frac{1}{2}(\lambda v)^2. \quad (13)$$

It is clear from the above equations that the Higgs sector of the NMSSM at tree-level is described by the six parameters:  $\lambda$ ,  $\kappa$ ,  $\tan \beta$ ,  $\mu_{\text{eff}}$ ,  $A_\lambda$  and  $A_\kappa$ . Assuming CP-conservation,

the upper mass bound for the lightest CP-even Higgs boson of the NMSSM, if it is the SM-like Higgs, at tree level is given by [8, 9]

$$m_{h_1}^2 < m_Z^2 \cos^2(2\beta) + \frac{\lambda^2 v^2}{2} \sin^2(2\beta). \quad (14)$$

The last term in this expression can lift  $m_{h_1}$  with up to 10-15 GeV higher than the corresponding one of the MSSM. So, less loop corrections are required to get the lightest Higgs,  $h_1$ , to be SM-like with mass around 125 GeV. Clearly, large values of  $\lambda$  and low values of  $\tan\beta$  are preferred to obtain a large value of the  $h_1$  at tree level. The scenarios with  $m_{h_1} < 125$  GeV means that the  $h_1$  is highly singlet-like so it can escape the constraints coming from LEP, the Tevatron and the LHC. In this case, the next-to-lightest CP-even Higgs boson  $h_2$  is the SM-like Higgs of mass around 125 GeV.

In this paper we are interested in the production of the next-to-lightest scalar Higgs boson  $h_2$ , which is not the SM-like Higgs, and its decays into either two light CP-odd Higgs bosons,  $a_1 a_1$ , or a light CP-odd Higgs and a gauge boson,  $a_1 Z$ , in the mass region  $m_{h_2} \lesssim 300$  GeV. We use the package NMSSMTools5.1.2 [59–61] which computes the masses, couplings and decay widths of all the Higgs bosons in addition to the spectrum of supersymmetric particles. This package takes into account various theoretical and experimental constraints such as constraints from negative Higgs searches at LEP, the Tevatron and the LHC, as well as SUSY mass limits as implemented in the package. Moreover, it takes into account constraints of Upsilon, B and K decays and also the bounds on the mass of the SM-like Higgs and its signal rates. More details about the constraints can be found on the website of the package. We have ignored the constraints on the dark matter because its nature is still unknown. We also do not take into account the constraints on the muon anomalous magnetic moment because such constraints have large theoretical uncertainties.

In our parameter space, we scan by varying the tree level parameters of the NMSSM within the following ranges:

$$\begin{aligned} 0.6 \leq \lambda \leq 0.7, & \quad -0.65 \leq \kappa \leq 0.65, & \quad 1.6 \leq \tan\beta \leq 60, \\ 100 \leq \mu_{\text{eff}} \leq 200 \text{ GeV}, & \quad -2000 \leq A_\lambda \leq 2000 \text{ GeV}, & \quad -10 \leq A_\kappa \leq 10 \text{ GeV}. \end{aligned}$$

Notice that we focus here on scenarios with large values of  $\lambda$  and small values of both  $\mu_{\text{eff}}$  and  $A_\kappa$  to simultaneously obtain the  $h_2$  with  $m_{h_2} \lesssim 300$  GeV and a light  $a_1$ . Remaining soft mass parameters for the scalars and gauginos in addition to the trilinear soft SUSY coupling parameters, contributing at higher order level, are set to

- $m_Q = m_U = m_D = m_L = m_E = m_{Q_3} = m_{U_3} = m_{D_3} = m_{L_3} = m_{E_3} = 3000$  GeV,
- $M_1 = 500$  GeV,  $M_2 = 1000$  GeV,  $M_3 = 3000$  GeV,
- $A_{U_3} = A_{D_3} = A_{E_3} = 3000$  GeV.

We randomly perform a scan over the above mentioned parameters and identify the parameter space of the NMSSM that passed all theoretical and experimental constraints. The outcome of our scan contains masses and branching ratios of the NMSSM Higgs bosons for all the surviving data points which have passed the constraints. As mentioned above, we have ignored the constraints on dark matter relic density. To know the effects of these constraints on the NMSSM parameter space see, for example, Ref. [62] and references therein.

### 3 Higgs boson signal rates

In this section we discuss the discovery potential of the  $h_2$  produced in the gluon fusion  $gg \rightarrow h_2$  at the LHC in the mass region  $m_{h_2} \lesssim 300$  GeV. The region with  $m_{h_2} \gtrsim 300$  GeV is less promising since the cross sections for the  $h_2$  production fall quickly with increasing  $h_2$  masses. For the surviving data points obtained from the random scan, we calculate the inclusive cross sections for the  $h_2$  production by using CalcHEP [63] for the following processes:

$$gg \rightarrow h_2 \rightarrow a_1 a_1 \rightarrow \tau^+ \tau^- \tau^+ \tau^- \quad \text{and} \quad gg \rightarrow h_2 \rightarrow Z a_1 \rightarrow \tau^+ \tau^- \tau^+ \tau^-. \quad (15)$$

Here, we consider a center-of-mass energy  $\sqrt{s} = 14$  TeV for the LHC.

In Fig. 1 we present the mass of the next-to-lightest CP-even Higgs boson  $m_{h_2}$  against the tree-level parameters of the NMSSM. One finds that for the surviving points the  $m_{h_2}$  decreases by increasing  $\lambda$  whereas it increases by increasing both  $\kappa$  and  $\mu_{\text{eff}}$ . Also, it is found that for our parameter space most of the surviving points correspond to the region with  $2 \lesssim \tan \beta \lesssim 7$  and  $200 \lesssim A_\lambda \lesssim 800$  while the distribution in  $A_\kappa$  is quite uniform.

Looking at Figs. 2 and 3, showing the correlations between  $m_{h_2}$  and the lightest CP-even Higgs mass  $m_{h_1}$  and between  $m_{h_2}$  and the lightest CP-odd Higgs mass  $m_{a_1}$  for the surviving points, it is clear that in most regions of our parameter space the  $h_1$  is the SM-like Higgs and the  $h_2$  can only play the role of the SM-like Higgs in a small region of the parameter space. The  $h_2$  is a mixture of doublet and singlet components for the majority of points selected in our parameter space. Fig. 3 shows that the smaller  $m_{a_1}$  the smaller  $m_{h_2}$ . Since the surviving points have small values of  $A_\kappa$ , only small values of  $m_{a_1}$  are allowed. One noteworthy feature of the figure is that the  $h_2$  can be the SM-like Higgs with mass around 125 GeV, which corresponds to a light  $a_1$  with  $m_{a_1} \lesssim 90$  GeV.

Due to the mixing between the Higgs doublets and singlet, Higgs-to-Higgs decays are kinematically allowed for large area of the NMSSM parameter space, even for small masses of Higgs bosons. Also, one distinguished landmark of the NMSSM is that the existence of the lightest CP-odd Higgs boson  $a_1$  with mass values less than  $m_Z$  is quite natural, which is impossible in the context of the MSSM. In Fig. 4 we display the correlations between  $m_{h_2}$  and the  $h_2$  decays into light CP-odd Higgs pairs  $h_2 \rightarrow a_1 a_1$  (left) and into an  $a_1$  and a gauge boson  $Z$  (right). It is clear from the left-panel of the figure that the decay  $h_2 \rightarrow a_1 a_1$  is the dominant one whenever it is kinematically open. It is found that the  $\text{BR}(h_2 \rightarrow a_1 a_1)$  ranges from around 40% to 100%, see the left-panel of the figure, while the maximum  $\text{BR}(h_2 \rightarrow Z a_1)$  is 0.1%, see the right-panel of the figure. In fact, the dominance of  $a_1 a_1$  decay channel causes a suppression to other decay channels such as  $b\bar{b}$  and other channels.

Fig. 5 illustrates the inclusive  $h_2$  production rates ending up with  $a_1 a_1 \rightarrow \tau^+ \tau^- \tau^+ \tau^-$  (left) and  $Z a_1 \rightarrow \tau^+ \tau^- \tau^+ \tau^-$  (right) as functions of  $m_{h_2}$ . It is shown from the figure that the  $h_2$  production rates decrease rapidly with increasing  $m_{h_2}$ . It is clear that the production rates  $\sigma(gg \rightarrow h_2 \rightarrow a_1 a_1 \rightarrow \tau^+ \tau^- \tau^+ \tau^-)$  are sizable, reaching up to 100 fb for small values of  $m_{h_2}$  while the production rates  $\sigma(gg \rightarrow h_2 \rightarrow Z a_1 \rightarrow \tau^+ \tau^- \tau^+ \tau^-)$  is quite small, reaching around 0.5 fb at the most. The latter production rates are clearly not enough to detect the  $h_2$  at the LHC, taking into account that leptonic tau decays are around 17.5%. In short, the

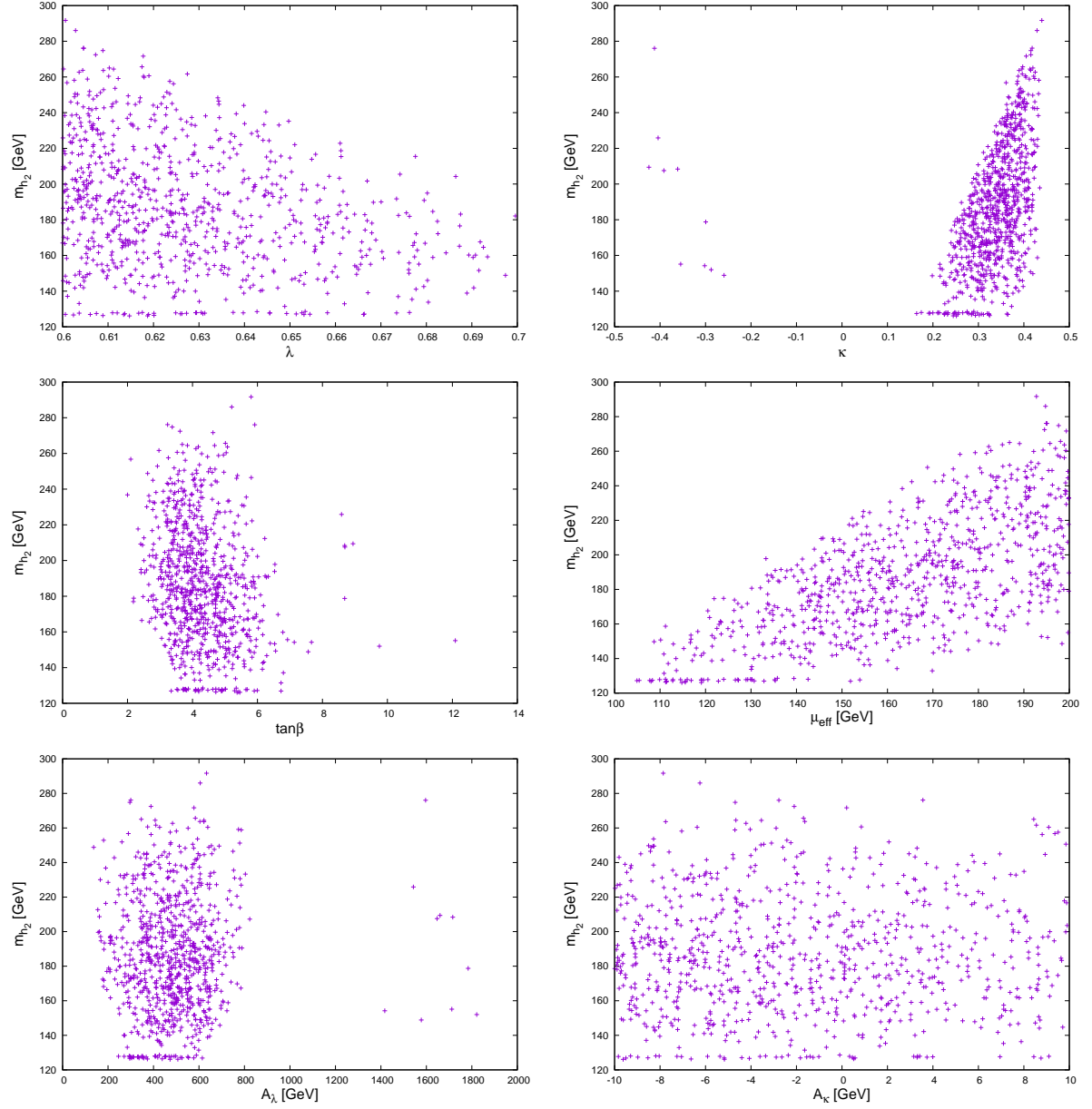


Figure 1: The next-to-lightest CP-even Higgs mass  $m_{h_2}$  as a function of  $\lambda$  and  $\kappa$  (top-panels),  $\tan\beta$  and  $\mu_{\text{eff}}$  (middle-panels) and  $A_\lambda$  and  $A_\kappa$  (bottom-panels).

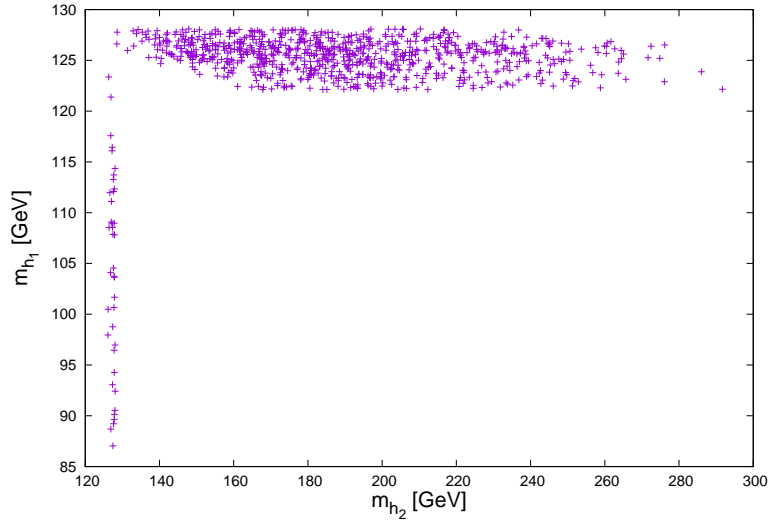


Figure 2: The mass distribution for the next-to-lightest CP-even Higgs,  $m_{h_2}$ , versus the lightest CP-even Higgs mass,  $m_{h_1}$ .

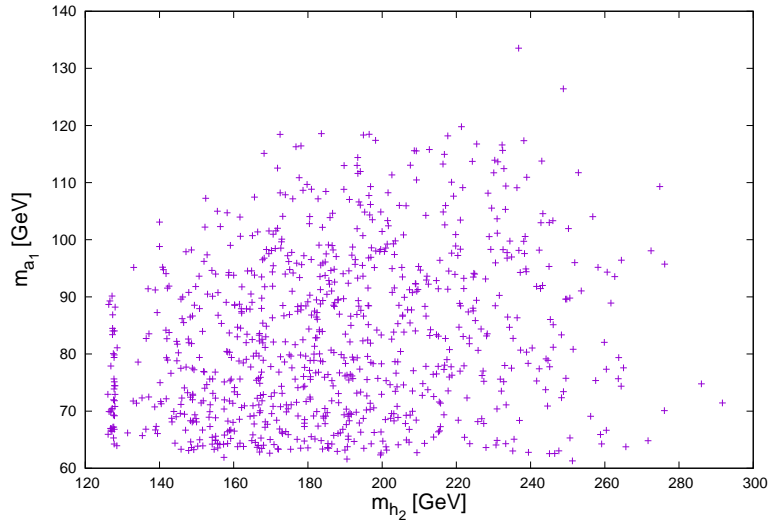


Figure 3: The mass distribution for the next-to-lightest CP-even Higgs,  $m_{h_2}$ , versus the lightest CP-odd Higgs mass,  $m_{a_1}$ .

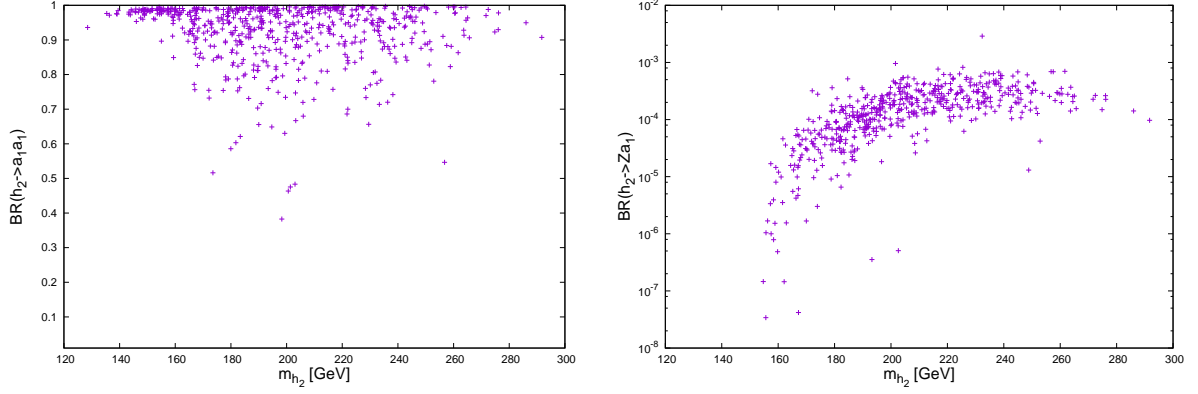


Figure 4: The next-to-lightest CP-even Higgs mass  $m_{h_2}$  plotted against both  $\text{BR}(h_2 \rightarrow a_1 a_1)$  (left) and  $\text{BR}(h_2 \rightarrow Z a_1)$  (right).

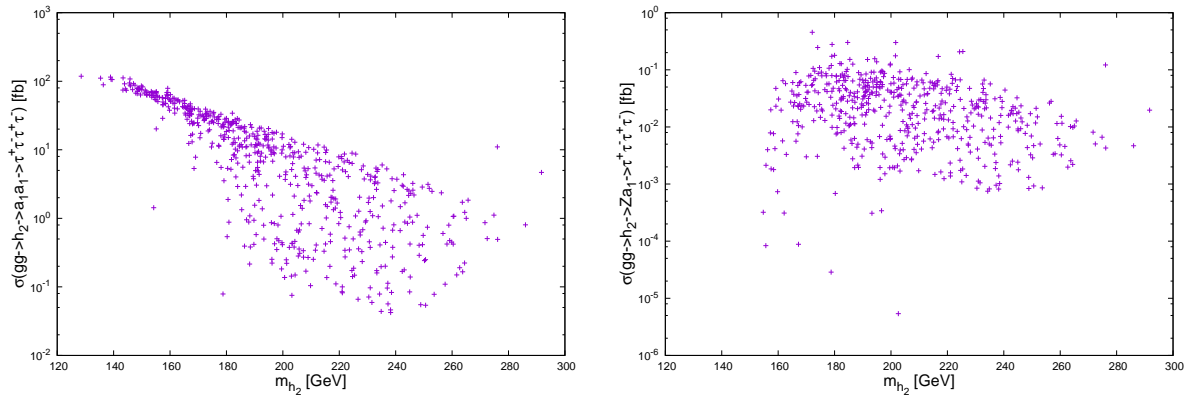


Figure 5: The production rates in fb for  $\sigma(gg \rightarrow h_2) \cdot \text{BR}(h_2 \rightarrow a_1 a_1 \rightarrow \tau^+ \tau^- \tau^+ \tau^-)$  (left) and  $\sigma(gg \rightarrow h_2) \cdot \text{BR}(h_2 \rightarrow Z a_1 \rightarrow \tau^+ \tau^- \tau^+ \tau^-)$  (right) as functions of  $m_{h_2}$ .



inclusive production rates for  $h_2$  decaying into  $a_1 a_1 \rightarrow \tau^+ \tau^- \tau^+ \tau^-$  are promising and could allow discovery of both  $h_2$  and  $a_1$  at the LHC while the production rates for  $h_2$  decaying into  $Z a_1 \rightarrow \tau^+ \tau^- \tau^+ \tau^-$  are quite small. So, we will analyze signal-to-background for the former channel as the latter channel is useless.

To claim discovery at the LHC, we have done a partonic signal-to-background (S/B) analysis based on CalcHEP. The dominant standard model backgrounds are the irreducible background coming from  $pp \rightarrow \tau^+ \tau^- \tau^+ \tau^-$  (via  $\gamma$  and  $Z$  exchange). Here, we assume the double leptonic decay channels of the  $\tau$ 's. In the table 1, we give 4 points as benchmark points for various masses of the  $h_2$  to do our analysis. Here, we assume that the tagging efficiency is 50% for tau -jets, by scaling of the total cross-sections. As it is shown in the table we have calculated the cross sections for both the signal and background processes and also the significance  $S/\sqrt{B}$  at a center-of-mass energy  $\sqrt{s} = 14$  TeV for the LHC. We have done that for  $300 \text{ fb}^{-1}$  and  $1000 \text{ fb}^{-1}$  of accumulated luminosity.<sup>2</sup> It is obvious that there is a good potential to detect the  $h_2$  decaying into  $a_1 a_1 \rightarrow \tau^+ \tau^- \tau^+ \tau^-$  at the LHC in the mass region  $140 \lesssim m_{h_2} \lesssim 220$  GeV. The corresponding signal events are quite large of order 31680 events for  $m_{h_2} = 140$  GeV and 2364 events for  $m_{h_2} = 220$  events with  $300 \text{ fb}^{-1}$  of integrated luminosity. Again these results given without assuming any cuts, which of course reducing the number of signal rates. Thus, we conclude that the LHC with integrated luminosity of  $1000 \text{ fb}^{-1}$  has the potential to discover the  $h_2$ , if it is not a SM-like Higgs, with masses up to around 250 GeV. Such a discovery of the  $h_2$  is mostly accompanied with a light  $a_1$ . The existence of such a light  $a_1$  is a direct evidence for distinguishing the NMSSM from the MSSM.

Table 1: Four benchmark points P1, P2, P3, and P4 used in the  $S/\sqrt{B}$  analysis.

	P1	P2	P3	P4
$\lambda$	0.615706	0.650828	0.637590	0.617789
$\kappa$	0.261287	0.264725	0.339134	0.387478
$\tan \beta$	5.2247	3.78738	3.82514	3.70979
$\mu_{\text{eff}} [\text{GeV}]$	153.678	198.766	198.201	199.224
$A_\lambda [\text{GeV}]$	646.778	517.464	464.215	426.835
$A_\kappa [\text{GeV}]$	-8.00937	5.1126	-9.72344	9.09329
$m_{h_2} [\text{GeV}]$	140	180	220	260
$m_{a_1} [\text{GeV}]$	66	64	99	67
$S$ [fb] with $300 \text{ fb}^{-1}$	$3.168 \times 10^4$	$8.61 \times 10^3$	$2.364 \times 10^3$	$3.21 \times 10^2$
$B$ [fb] with $300 \text{ fb}^{-1}$	$3.9 \times 10^4$	$3.9 \times 10^4$	$3.9 \times 10^4$	$3.9 \times 10^4$
$S/\sqrt{B}$ with $300 \text{ fb}^{-1}$	160.4	43.6	12	1.6
$S/\sqrt{B}$ with $1000 \text{ fb}^{-1}$	292.9	79.6	21.9	3

<sup>2</sup>We do such analysis without assuming any cuts. Of course, the proper cuts could improve the signal to background ratio, which we leave for the experimentalist to do.

## 4 Conclusions

In this paper, we have explored the discovery prospects of the next-to-lightest CP-even Higgs state,  $h_2$ , at the LHC with  $\sqrt{s} = 14$  TeV. We have studied the detectability of the  $h_2$  in the two processes  $gg \rightarrow h_2 \rightarrow a_1 a_1 \rightarrow \tau^+ \tau^- \tau^+ \tau^-$  and  $gg \rightarrow h_2 \rightarrow Z a_1 \rightarrow \tau^+ \tau^- \tau^+ \tau^-$ . We have shown that while the  $h_2$  discovery of the latter channel is impossible due to smallness of the inclusive production rates, the former channel is promising as the  $\sigma(gg \rightarrow h_2 \rightarrow a_1 a_1 \rightarrow \tau^+ \tau^- \tau^+ \tau^-)$  is sizable, and should help discovering the  $h_2$  signals with masses up to around 250 GeV at the LHC with integrated luminosity of  $1000 \text{ fb}^{-1}$ .

After doing some analysis for signals and dominant backgrounds in the partonic level, we have proven that the discovery of both the  $h_2$  and  $a_1$  are possible at the LHC. Such a discovery of the  $h_2$  is mostly accompanied with a light  $a_1$  with  $m_{a_1} \lesssim m_Z$ . The existence of such a light  $a_1$  is a direct evidence for the NMSSM as such a light  $a_1$  is impossible in the MSSM. Of course, more experimental analysis including  $\tau$ -decays, detector effects, parton shower, and hadronization are needed to claim the actual discovery potential of such Higgses at the LHC. However, we believe that our results are valuable for scientists interested in determining the NMSSM Higgs signals at the LHC.

The discovery of Higgs states through the process  $gg \rightarrow h_2 \rightarrow a_1 a_1 \rightarrow \tau^+ \tau^- \tau^+ \tau^-$  has in fact two merits. On the one hand, it can be a good alternative to discover both  $h_2$  and  $a_1$  that could be difficult to be discovered in direct production. On the other hand, it can be exploited to measure the trilinear Higgs self-coupling  $h_2 a_1 a_1$ .

## Acknowledgments

We gratefully acknowledge support of Taibah University, KSA.

## References

- [1] S. Chatrchyan *et al.* [CMS Collaboration], Phys. Lett. B **716**, 30 (2012).
- [2] G. Aad *et al.* [ATLAS Collaboration], Phys. Lett. B **716**, 1 (2012).
- [3] S. Chatrchyan *et al.* [CMS Collaboration], JHEP **1306**, 081 (2013).
- [4] G. Aad *et al.* [ATLAS Collaboration], Phys. Lett. B **726**, 88 (2013).
- [5] H. P. Nilles, M. Srednicki and D. Wyler, Phys. Lett. B **120**, 346 (1983).
- [6] J. M. Frere, D. R. T. Jones and S. Raby, Nucl. Phys. B **222**, 11 (1983).
- [7] J. P. Derendinger and C. A. Savoy, Nucl. Phys. B **237**, 307 (1984).
- [8] J. R. Ellis, J. F. Gunion, H. E. Haber, L. Roszkowski and F. Zwirner, Phys. Rev. D **39**, 844 (1989).

- [9] M. Drees, *Int. J. Mod. Phys. A* **4**, 3635 (1989).
- [10] U. Ellwanger, M. Rausch de Traubenberg and C. A. Savoy, *Phys. Lett. B* **315**, 331 (1993).
- [11] S. F. King and P. L. White, *Phys. Rev. D* **52**, 4183 (1995).
- [12] F. Franke and H. Fraas, *Int. J. Mod. Phys. A* **12**, 479 (1997).
- [13] U. Ellwanger, M. Rausch de Traubenberg and C. A. Savoy, *Nucl. Phys. B* **492**, 21 (1997).
- [14] M. Masip, R. Muñoz-Tapia and A. Pomarol, *Phys. Rev. D* **57** 5340 (1998).
- [15] M. Maniatis, *Int. J. Mod. Phys. A* **25** 3505 (2010).
- [16] U. Ellwanger, C. Hugonie and A. M. Teixeira, *Phys. Rept.* **496**, 1 (2010).
- [17] J. E. Kim and H. P. Nilles, *Phys. Lett. B* **138**, 150 (1984).
- [18] U. Ellwanger, J.F. Gunion, C. Hugonie and S. Moretti, hep-ph/0305109.
- [19] U. Ellwanger, J. F. Gunion and C. Hugonie, *JHEP* **0507** 041 (2005).
- [20] S. Moretti, S. Munir and P. Poulose, *Phys. Lett. B* **644** 241 (2007).
- [21] J. R. Forshaw, J. F. Gunion, L. Hodgkinson, A. Papaefstathiou and A. D. Pilkington, *JHEP* **0804** 090 (2008).
- [22] A. Belyaev, J. Pivarski, A. Safonov, S. Senkin and A. Tatarinov, *Phys. Rev. D* **81** 075021 (2010).
- [23] M. M. Almarashi and S. Moretti, *Eur. Phys. J. C* **71** 1618 (2011).
- [24] M. M. Almarashi and S. Moretti, *Phys. Rev. D* **83** 035023 (2011).
- [25] M. M. Almarashi and S. Moretti, *Phys. Rev. D* **84** 015014 (2011).
- [26] M. M. Almarashi and S. Moretti, *Phys. Rev. D* **84**, 035009 (2011).
- [27] F. Mahmoudi, J. Rathsman, O. Stal and L. Zeune, *Eur. Phys. J. C* **71** 1608 (2011).
- [28] Z. Kang, J. Li, T. Li, D. Liu and J. Shu, *Phys. Rev. D* **88**, no.1, 015006 (2013).
- [29] D. G. Cerdeno, P. Ghosh and C. B. Park, *JHEP* **06**, 031 (2013).
- [30] J. Cao, Z. Heng, L. Shang, P. Wan and J. M. Yang, *JHEP* **04**, 134 (2013).
- [31] N. D. Christensen, T. Han, Z. Liu and S. Su, *JHEP* **08**, 019 (2013).
- [32] U. Ellwanger, *JHEP* **08**, 077 (2013).

- [33] D. G. Cerdeño, P. Ghosh, C. B. Park and M. Peiro, JHEP **02**, 048 (2014).
- [34] S. F. King, M. Muhlleitner, R. Nevzorov and K. Walz, Phys. Rev. D **90**, no. 9, 095014 (2014).
- [35] N. E. Bomark, S. Moretti, S. Munir and L. Roszkowski, JHEP **1502**, 044 (2015).
- [36] A. Chakraborty, D. K. Ghosh, S. Mondal, S. Poddar and D. Sengupta, Phys. Rev. D **91**, 115018 (2015).
- [37] U. Ellwanger and M. Rodriguez-Vazquez, JHEP **02**, 096 (2016).
- [38] U. Ellwanger and C. Hugonie, JHEP **1605**, 114 (2016).
- [39] E. Conte, B. Fuks, J. Guo, J. Li and A. G. Williams, JHEP **1605**, 100 (2016).
- [40] F. Wang, W. Wang, L. Wu, J. M. Yang and M. Zhang, Int. J. Mod. Phys. A **32**, no.33, 1745005 (2017).
- [41] M. Guchait and J. Kumar, Phys. Rev. D **95**, no. 3, 035036 (2017).
- [42] S. P. Das and M. Nowakowski, Phys. Rev. D **96**, no.5, 055014 (2017).
- [43] C. Beskidt, W. de Boer and D. I. Kazakov, Phys. Lett. B **782**, 69 (2018).
- [44] M. M. Almarashi, Results Phys. **10**, 799 (2018).
- [45] M. M. Almarashi, Int. J. Mod. Phys. A **33**, no.10, 1850071 (2018).
- [46] Z. Heng, X. Gong and H. Zhou, Chin. Phys. C **42**, no.7, 073103 (2018).
- [47] S. P. Das, J. Fraga and C. Avila, Int. J. Mod. Phys. A **34**, no.22, 1950125 (2019).
- [48] D. Das, Phys. Rev. D **99**, no.9, 095035 (2019).
- [49] S. Baum, N. R. Shah and K. Freese, JHEP **04**, 011 (2019).
- [50] K. Wang and J. Zhu, JHEP **06**, 078 (2020).
- [51] M. M. Almarashi, Int. J. Mod. Phys. A **35**, no.25, 2050151 (2020).
- [52] R. Dermisek and J. F. Gunion, Phys. Rev. Lett. **95** 041801 (2005).
- [53] A. Belyaev, S. Hesselbach, S. Lehti, S. Moretti, A. Nikitenko and C. H. Shepherd-Themistocleous, [arXiv:0805.3505 [hep-ph]].
- [54] M. Lisanti and J.G. Wacker, Phys. Rev. D **79** 115006 (2009).
- [55] M. M. Almarashi and S. Moretti, Phys. Rev. D **85**, 017701 (2012).
- [56] R. D. Peccei and H. R. Quinn, Phys. Rev. Lett. **38**, 1440 (1977).

- [57] R. D. Peccei and H. R. Quinn, Phys. Rev. D **16**, 1791 (1977).
- [58] D.J. Miller, R. Nevzorov and P.M. Zerwas, Nucl. Phys. B **681**, 3 (2004).
- [59] U. Ellwanger, J.F. Gunion and C. Hugonie, JHEP **0502**, 066 (2005).
- [60] U. Ellwanger and C. Hugonie, Comput. Phys. Commun. **175**, 290 (2006).
- [61] See <http://www.th.u-psud.fr/NMHDECAY/nmssmtools.html>.
- [62] E. Aldufeery and M. Binjonaid, Universe **7**, no.2, 31 (2021).
- [63] A. Pukhov, arXiv:hep-ph/0412191.